Pro-Apoptotic Protein Noxa Regulates Memory T Cell Population Size and Protects against Lethal Immunopathology

Wensveen, F. M.; Klarenbeek, P. L.; van Gisbergen, K. P. J. M.; Pascutti, M. F.; Derks, I. A. M.; van Schaik, B. D. C.; ten Brinke, A.; de Vries, N.; Cekinović, Đurđica; Jonjić, Stipan; ...

Source / Izvornik: **The Journal of Immunology, 2012, 190, 1180 - 1191**

Journal article, Published version
Rad u časopisu, Objavljena verzija rada (izdavačev PDF)

https://doi.org/10.4049/jimmunol.1202304

Permanent link / Trajna poveznica: https://urn.nsk.hr/urn:nbn:hr:184:924563

The Journal of Immunology

Pro-Apoptotic Protein Noxa Regulates Memory T Cell Population Size and Protects against Lethal Immunopathology

Felix M. Wensveen, Paul L. Klarenbeek, Klaas P. J. M. van Gisbergen, Maria F. Pascutti, Ingrid A. M. Derks, Barbera D. C. van Schaik, Anja ten Brinke, Niek de Vries, Durdica Cekinovic, Stipan Jonjic, René A. W. van Lier and Eric Eldering

J Immunol 2013; 190:1180-1191; Prepublished online 31 December 2012;
doi: 10.4049/jimmunol.1202304
http://www.jimmunol.org/content/190/3/1180

The Journal of Immunology is published twice each month by
The American Association of Immunologists, Inc.,
1451 Rockville Pike, Suite 650, Rockville, MD 20852

Print ISSN: 0022-1767 Online ISSN: 1550-6606.

Pro-Apoptotic Protein Noxa Regulates Memory T Cell Population Size and Protects against Lethal Immunopathology

Felix M. Wensveen,* Paul L. Klarenbeek,*,† Klaas P. J. M. van Gisbergen,*,‡ Maria F. Pascutti,*,§ Ingrid A. M. Derks,* Barbera D. C. van Schaik,¶ Anja ten Brinke,‖ Niek de Vries,† Đurđica Cekinović,# Stipan Jonjić,# René A. W. van Lier,*,‡ and Eric Eldering*

Memory T cells form a highly specific defense layer against reinfection with previously encountered pathogens. In addition, memory T cells provide protection against pathogens that are similar, but not identical to the original infectious agent. This is because each T cell response harbors multiple clones with slightly different affinities, thereby creating T cell memory with a certain degree of diversity. Currently, the mechanisms that control size, diversity, and cross-reactivity of the memory T cell pool are incompletely defined. Previously, we established a role for apoptosis, mediated by the BH3-only protein Noxa, in controlling diversity of the effector T cell population. This function might positively or negatively impact T cell memory in terms of function, pool size, and cross-reactivity during recall responses. Therefore, we investigated the role of Noxa in T cell memory during acute and chronic infections. Upon influenza infection, Noxa$^{-/-}$ mice generate a memory compartment of increased size and clonal diversity. Reinfection resulted in an increased recall response, whereas cross-reactive responses were impaired. Chronic infection of Noxa$^{-/-}$ mice with mouse CMV resulted in enhanced memory cell inflation, but no obvious pathology. In contrast, in a model of continuous, high-level T cell activation, reduced apoptosis of activated T cells rapidly led to severe organ pathology and premature death in Noxa-deficient mice. These results establish Noxa as an important regulator of the number of memory cells formed during infection. Chronic immune activation in the absence of Noxa leads to excessive accumulation of primed cells, which may result in severe pathology. ***The Journal of Immunology*****, 2013, 190: 1180–1191.**

After a pathogen has been successfully cleared from the body, the adaptive immune system forms immunological memory cells that provide long-lasting protection against reinfection. Sufficient numbers of memory cells must be formed to counter the reinfecting agent in a short enough time to prevent its spread and replication, to achieve efficient protection. In contrast, the maximum size of the memory cell pool must be restricted to prevent excessive immune activation and pathology upon reinfection (1). In addition to population size, clonal diversity of the memory cell pool must be controlled to ensure appropriate effectiveness of recall responses. Previously, it has been shown that clonal diversity of the memory cell pool roughly reflects that of the effector cell response, suggesting strong clonal selection (2). However, a too restricted specificity of the memory cell pool appears to be counterproductive (3). As many pathogens, such as HIV and seasonal influenza, rapidly accumulate point mutations, they may no longer be recognized by the memory cell pool when the number of epitopes that is recognized is too small. Indeed, studies both in humans and mice indicate that increased clonal diversity of the memory cell pool provides enhanced protection (4, 5). Mechanisms are therefore in place to ensure an appropriate size of the memory pool, whereas maintaining a certain level of diversity.

Proper control of cell death plays an important role in the control of memory T cell formation and reactivation (6, 7). Both death-receptor–mediated apoptosis and the mitochondrial or intracellular cell death pathway have been implicated in memory T cell biology (8, 9). Deregulation of cell death pathways greatly affects the number of memory T cells formed. Mice deficient for proapoptotic Bim and Fas accumulate large numbers of memory T cells after lymphocytic choriomeningitis virus infection (10, 11). Upregulation of Bcl-2 is essential for IL-7–mediated memory T cell survival (12). The role that other proapoptotic and antiapoptotic molecules play in memory cell survival remains relatively unknown.

A prominent candidate that potentially regulates memory cell formation is the pro-apoptotic protein Noxa (encoded by *Pmaip1*). During priming in the lymph node (LN), T cell activation, sur-

*Department of Experimental Immunology, Academic Medical Center, University of Amsterdam, 1105 AZ Amsterdam, The Netherlands; †Department of Clinical Immunology and Rheumatology, Academic Medical Center, University of Amsterdam, 1105 AZ Amsterdam, The Netherlands; ‡Department of Hematopoiesis, Sanquin Research, 1066 CX Amsterdam, The Netherlands; §Department of Hematology, Academic Medical Center, University of Amsterdam, 1105 AZ Amsterdam, The Netherlands; ¶Department of Clinical Epidemiology Biostatistics and Bioinformatics, Academic Medical Center, University of Amsterdam, 1105 AZ Amsterdam, The Netherlands; ‖Department of Immunopathology, Sanquin Research, 1066 CX Amsterdam, The Netherlands; and #Department of Histology and Embryology, University of Rijeka, HR-51000 Rijeka, Croatia

Received for publication August 16, 2012. Accepted for publication November 21, 2012.

This work was supported by a Vici grant of The Netherlands Organisation for Scientific Research (to R.A.W.v.L. and K.P.J.M.v.G.) and Academic Medical Center graduate school scholarships (to F.M.W. and P.L.K.).

Address correspondence and reprint requests to Dr. Felix M. Wensveen, Braće Branchetta 20, 51000 Rijeka, Croatia. E-mail address: Felix.Wensveen@gmail.com

Abbreviations used in this article: B6, C57BL/6J; CFSE, carboxyfluorescein succinimidyl ester; DDAO, 7-hydroxy-9H-(1,3-dichloro-9,9-dimethylacridin-2-one); LN, lymph node; mCMV, mouse CMV; MFI, mean fluorescent intensity; PR8, influenza A/PR/8/34; RT-MLPA, multiplex ligation-dependent probe amplification; SLEC, short-lived effector cell; WT, wild-type.

www.jimmunol.org/cgi/doi/10.4049/jimmunol.1202304

vival, and effector pool size are strictly limited by the availability of Ag, costimulatory molecules, nutrients, and cytokines (13). Even in the presence of all these factors, outgrowth of some activated T cells is favored over others, based on TCR affinity (14). Previously, we have shown that expansion and persistence of low-affinity effector cells is inhibited via competition-based apoptosis that mediates clonal dominance of high-affinity clones via the termination of low-affinity T cells (15). TCR affinity influences stability of the prosurvival molecule Mcl-1 via an IL-2R–mediated signaling loop. T cells lacking Noxa, the antagonist of Mcl-1 (16), therefore have a competitive advantage during priming, resulting in the survival and recruitment of increased numbers of low-affinity clones into the effector cell pool. This results in decreased numbers of high-affinity cells and reduced Ag responsiveness of the effector T cell pool as a whole. Currently, it is unknown whether Noxa mediates similar effects during the formation of memory T cells.

In this study, we investigated how the absence of Noxa affects the formation, maintenance, and recall capabilities of memory T cells. We find that Noxa ablation results in enhanced diversity of the memory cell compartment and increased absolute memory cell numbers upon influenza infection. As a result of increased memory cell numbers, Noxa$^{-/-}$ mice form enlarged recall responses and have increased memory inflation during chronic mouse CMV (mCMV) infection. In a transgenic model of persistent T cell activation, effector T cell accumulation ultimately led to severe organ pathology and premature death in mice deficient for Noxa. Our data show that control of memory precursor (MP) cell numbers via Noxa-mediated apoptosis is essential to prevent excessive immune responses upon reinfection.

Materials and Methods

Mice

C57BL/6J (B6) and B6 Ly5.1$^+$ (B6.SJL-Ptprca Pepcb/BoyJ) JAX mice were purchased from Charles River and kept as breeding colonies in our local animal facility. Only these mice, which were kept under identical conditions as our transgenic and gene-targeted mice, were used as wild-type (WT) controls in our experiments. Noxa$^{-/-}$ mice (C57BL/6-Pmaip1tm1Ast/J) were a kind gift from Dr. A. Strasser (Walter and Eliza Hall Institute, Melbourne, Australia) and provided by Dr. M. Serrano (Spanish National Cancer Research Centre, Madrid, Spain). Noxa5.1 mice were generated by crossing Noxa$^{-/-}$ mice with B6 Ly5.1$^+$ mice from our in-house colony. B cell–specific CD70^{TG} mice were generated as previously described (17). Noxa70 mice were generated by crossing Noxa$^{-/-}$ mice with CD70^{TG} mice. Mice were used at 6–12 wk of age, unless stated otherwise, were age and sex matched within experiments, and were handled in accordance with institutional and national guidelines. All mice were either generated in B6 mice or backcrossed at least 10 times on this background.

Viral infection

Influenza A virus strains used were A/PR/8/34 (PR8, H1N1) (18), A/Aichi/HK/2/68 (HK2/68, H3N2) (19), and A/HKx31 (HKx31, H2N3; this is a recombinant of the PR8 and HK2/68 strains) (20). Viruses were generated in LLC-MK2 cells, and 50% tissue culture-infective dose was determined in WT B6 mice as previously described (21). Mice were infected intranasally with 10 × 50% tissue culture-infective dose under general anesthesia. Bacterial artificial chromosome–derived mCMV strain MW97.01, which was experimentally shown to be identical to the WT Smith strain (22), was generated in primary mouse embryonic fibroblasts according to standard protocol (23). PFUs were determined by standard plaque assay on mouse embryonic fibroblasts, and 5×10^5 PFUs per mouse were injected i.p.

Flow cytometry

Single-cell suspensions were obtained by mincing the specified organs through 40-μm cell strainers (Becton Dickinson). Erythrocytes were lysed with an ammonium chloride solution (155 mM NH4Cl, 10 mM $KHCO_3$, and 1 mM EDTA), and cells were subsequently counted using an automated cell counter (Schärfe System). Cells (5×10^5 to 5×10^6) were collected in staining buffer (PBS with 0.5% BSA; Sigma) and stained for 30 min at 4˚C with Abs in the presence of anti-CD16 and anti-CD32 (clone 2.4G2), anti-mouse FcγRII and FcγRIII (a kind gift of Louis Boon, Bioceros, Utrecht, The Netherlands). mAbs against CD3 (145-2C11), CD4 (L3T4), and CD62L (Mel-14) were bought from BD Biosciences. Abs against CD8 (53.6.7), CD44 (IM7), CD45.1 (A20), CD127 (A7R34), IFN-γ (XMG1.2), and KLRG1 (2F1) were bought from eBiosciences. FACS experiments were performed on a FACSCalibur or FACSCanto (Becton Dickinson) and analyzed with FlowJo software (TriStar). T cell subsets were sorted to >99% purity with a FACSAria (Becton Dickinson). PE- or allophycocyanin-conjugated H2D^b and H2K^b tetramers were made by Sanquin (http://www.sanquin.nl). To stain influenza-specific CD8 T cells, we loaded H2D^b tetramers with ASNENMETM (D^{b}METM; HKx31 and PR8) or ASNENMDAM (D^{b}MDAM; HK2/68). To stain mCMV-specific cells, we loaded H2K^b tetramers with SCLEFWQRV (K^{b}m57), TVYGFCLL (K^{b}m139), and RALEYKNL (K^{b}mIE3).

Multiplex ligation-dependent probe amplification analysis

Total RNA was extracted using the TRIzol isolation method (Invitrogen). mRNA levels were analyzed with the Apoptosis Mouse mRNA multiplex ligation-dependent probe amplification (RT-MLPA) kit (MRC-Holland, http://www.mlpa.com) according to the manufacturer's instructions. Samples were run through a GeneScan and analyzed with GeneMapper (Applied Biosystems GmbH; http://www.appliedbiosystems.com) and subsequently Excel software (Microsoft) as described previously (15).

Flow cytometric measurement of intracellular proteins

To determine direct ex vivo cytokine production, we plated splenocytes at 1×10^6 cells/well in a 96-well round-bottom plate and stimulated with 10 ng/ml PMA and 1 μM ionomycin (Sigma) or with peptides (ASNENMETM, SCLEFWQRV, RALEYKNL, and TVYGFCLL; Genscript, http://www.genscript.com) for 6 h at 37˚C. During the final 4 h, 1 μg/ml of the protein-secretion inhibitor brefeldin A (Sigma) was added. Thereafter, cells were washed and stained with anti-CD4 or anti-CD8, followed by fixation and permeabilization (Becton Dickinson). Cells were then incubated for 30 min with fluorescently labeled Abs against IFN-γ, thoroughly washed, and analyzed by flow cytometry.

Adoptive transfer and in vivo cytotoxicity

For adoptive transfer, WT and Noxa$^{-/-}$ mice (both CD45.1) were infected intranasally with influenza PR8. Ten days postinfection, CD8$^+$ T cells were isolated from spleens by positive selection using the MACS cell separation system (Miltenyi). Cells were injected i.v. in WT (CD45.2) recipient mice, and contraction was followed in the blood. For in vivo cytotoxicity (see Fig. 3C), splenocytes from naive WT (CD45.1) mice were isolated, divided in four fractions, and labeled with carboxyfluorescein succinimidyl ester (CFSE), 7-hydroxy-9H-(1,3-dichloro-9,9-dimethylacridin-2-one) (DDAO) (both Molecular Probes), both, or nothing. Fractions were subsequently incubated for 2 h with the viral peptides ASNENMETM (CFSE$^+$), SSLENFRAYV (DDAO$^+$), and LSLRNPILV (CFSE$^+$DDAO$^+$) or the control peptide SIINFEKL (no dye) in RPMI, washed, and mixed in a 1:1:1:1 ratio. A total of 10×10^6 cells of this mixture was injected per mouse in WT or Noxa$^{-/-}$ recipients (CD45.2) that had been infected with influenza 50 d previously. As a readout for specific killing, the relative decrease of viral-peptide pulsed cells, in comparison with control-peptide pulsed cells, was measured within the CD45.1$^+$ cell pool in the blood.

PCR and sequence analysis of TCR clones

Total RNA was extracted from CD3$^+$CD4$^-$CD8$^+$D^{b}METM$^+$ T cells, sorted with a FACSAria (BD Biosciences) cell sorter, using the TRIzol (Invitrogen) isolation method, according to the manufacturer's protocol. cDNA was generated using SuperscriptII-RT and oligo-dT primers according to the manufacturer's protocol (#18064; Invitrogen). The CDR3 of the β-chain was used as a unique tag for clonal expansions, as previously described (3, 24). The TCR of the D^{b}METM tetramer binding cells were amplified with primers specific for the Vβ8.3 gene segment (5′-GCCTCCCTCGCGCCATCA GTGCTGGCAACCTTCGAATAGGA-3′) and the Constant segment (5′-AAGGAGACCTTGGGTGGAGT-3′), using the following PCR conditions: 4 μl cDNA (out of a total volume of 50 μl) was amplified in the presence of 10 pmol of both primers, 1 mM MgCL2, 0.1 mM dNTPs, 1× Buffer B (Solis BioDyne, Tartu, Estonia), and 2 U Hotfire-Polymerase (Solis BioDyne) in a volume of 40 μl. Amplification was performed on a T3000 thermocycler (Biometra, Göttingen, Germany) in 35 cycles (hot start [96˚C for 15 min], then 40× [96˚C for 30 s, 60˚C for 1 30 s, 72˚C for

60 s], and 10 min at 72°C). Amplification products were purified using AMPure SPRI beads (Agencourt Bioscience, Beverly, MA). The primers were tailed with the primer A and primer B sequences that allow high-throughput sequencing using a Genome Sequencer FLX (Roche Diagnostics, Mannheim, Germany). CDR3 regions were identified as described earlier (24). Preparation of the samples and sequencing was performed according to the manufacturer's protocol for amplicon sequencing on the FLX platform.

Immunohistochemistry

For histochemical analysis, formalin-fixed and paraffin-embedded sections were stained with H&E. For immunohistochemical analysis, sections were stained with primary Abs against cleaved caspase-3 (Cell Signaling) and subsequently with PowerVision Anti-Rabbit Poly-HRP (Immunologic). Cells were visualized with diaminobenzidine (Sigma-Aldrich) and counterstained with hematoxylin.

Statistical analysis

Statistical analysis of the data were performed using the unpaired Student *t* test, Wilcoxon Mantel–Cox test, one-way ANOVA test, or Mann–Whitney *U* test where applicable. Asterisks denote significant differences ($*p < 0.05$, $**p < 0.005$, $***p < 0.0005$).

Results

Noxa limits CD8$^+$ memory T cell numbers

Previously, we observed Noxa induction after in vitro stimulation of naive CD8 T cells (15, 25). To investigate whether Noxa may also be expressed during memory T cell formation, we analyzed mRNA levels of Noxa and 39 other apoptosis genes ex vivo in CD8 T cell subpopulations. Mice were infected with PR8 virus and 10 days later, splenic short-lived effector cells (SLECs) and MP cells were sorted. mRNA expression was compared with that of naive T cells and central memory (CM) cells via RT-MLPA analysis. For the prosurvival Bcl-2 proteins, expression of Bcl-XL was higher in all Ag-experienced T cell subsets compared with naive cells (Fig. 1A). In accordance with previous findings, specifically SLECs had reduced levels of Bcl-2 (26). Interestingly, prosurvival molecule BCL2A1 and its antagonist Noxa, which we and others had previously shown to be induced in activated T cells (15, 25, 27), are also highly expressed in MP cells, whereas their mRNA levels are lower in central memory cells. mRNA expression of Puma, in contrast, followed a reciprocal pattern, and its expression is higher in central memory cells (Fig. 1A).

The similar high level of Noxa expression in MPs as in SLECs prompted us to investigate memory cell formation in Noxa-deficient mice. WT and Noxa$^{-/-}$ mice were infected with influenza A/HKx31 (HKx31) or PR8, and memory cell formation was followed over time. As previously described (15), size and affinity of the Ag-specific effector cell pool was reduced in Noxa-deficient animals. At the peak of infection, less D^{b}METM$^+$ CD8 T cells were observed in the blood of Noxa$^{-/-}$ mice (Fig. 1B). In addition, the mean fluorescent intensity (MFI) of tetramer binding, which was previously shown to be a reliable measure of TCR affinity (15), was reduced in Noxa$^{-/-}$ effector cells (Fig. 1C). Interestingly, at this time point postinfection, no differences in numbers or tetramer binding were observed between MP populations (Fig. 1C). In contrast, D^{b}METM$^+$ CD8 T cell numbers were increased in Noxa$^{-/-}$ mice after 1 mo of infection and at later time points. At these time points, most influenza-specific SLECs has died and almost all cells have a CD127$^+$KLRG1$^-$ memory phenotype (28). Indeed, Noxa-deficient mice had increased numbers of flu-specific CD8 T cells displaying a memory phenotype at late time points postinfection, whereas no differences in the number of SLECs were observed (Fig. 1D, 1E). The increase in flu-specific central and effector memory populations was also observed in the spleen and mediastinal LN of Noxa$^{-/-}$ mice (Fig. 1F, 1G), suggesting that Noxa restricts memory cell numbers within secondary lymphoid tissues. To investigate whether maintenance of memory cells was affected, we quantified decay of Ag-specific cells between days 28 and 66 post-infection. The $t_{1/2}$ of Ag-specific cells was not significantly different between WT and Noxa$^{-/-}$ cells (WT: 71 ± 33 d, Noxa$^{-/-}$: 89 ± 30 d; $p = 0.58$), indicating that Noxa deficiency affects memory formation, rather than memory cell maintenance at later time points.

To investigate whether Noxa impacts recall responses, we performed a challenge experiment, as previously described (29). WT and Noxa-deficient mice were infected intranasally with the influenza strain HKx31. This virus is a recombinant that expresses the internal components of PR8, but the cell surface proteins of A/Aichi/HK/2/68 (HK2/68) (20). Therefore, reinfection with PR8 induces a strong memory CD8 T cell response, whereas no Abs recognize this virus. Two months after HKx31 infection, animals were reinfected with PR8 and CD8 T cell responses were analyzed after 9 d. Noxa$^{-/-}$ mice generated an Ag-specific CD8 T cell response that was significantly larger than that of WT mice, both in spleen and lungs (Fig. 1H). However, both before and after reinfection, Noxa$^{-/-}$ mice had roughly two times more Ag-specific cells within their CD8 T cell pool. This suggests that the increased recall response in Noxa-deficient mice is solely the result of increased memory cell numbers and not of *per cell* differences in recall capacity. Thus, Noxa limits the size of the memory pool, and thereby the size of the CD8 T cell recall response.

Noxa contributes to selection of CD8$^+$ T cell clones during primary but not secondary responses

Previously, we have shown that Noxa mediates selection of high-affinity clones during primary effector responses (15). Enhanced survival of subdominant clones may therefore be responsible for the increase in memory cells in Noxa$^{-/-}$ mice. To examine whether Noxa also affected selection of clones in memory and recall responses, we analyzed the clonal diversity of D^{b}METM$^+$ CD8 T cells. WT and Noxa-deficient mice were infected with influenza PR8 virus, and D^{b}METM$^+$ CD8 T cells were sorted after 84 d. Clonal TCR analysis was performed using next generation sequencing. CDR3 regions were compared in T cells that use the Vβ8.3 gene fragment (3, 24). The response against the ASNENMETM epitope is dominated by a Vβ8.3-restricted population containing many public clones, which allows direct comparison (30).

On average 6194 (±409) Vβ8.3 sequences were analyzed per animal. Clones retrieved less than three times were excluded from analysis, to prevent "pollution" with naive clones. In both groups, the majority of reads was derived from a limited number of expanded clones (sequences retrieved >50 times). Together, 750 clones were detected in Noxa$^{-/-}$ mice, compared with only 368 clones in WT animals. In line with these findings, the median frequency of clones in Noxa$^{-/-}$ mice was significantly lower compared with that in WT mice (Fig. 2A). Further analysis revealed that this difference was primarily caused by an increase of low-frequency clones (3–11 copies/clone; Fig. 2B).

Next, the diversity of the recall populations was compared between WT and Noxa$^{-/-}$ mice. Mice were infected with influenza HKx31 and reinfected with PR8 after 2 mo. D^{b}METM$^+$ CD8 T cells were sorted after 9 d, and Vβ8.3 T cells were analyzed by deep sequencing. Strikingly, the clonal variety within the CD8 T cell population was very much reduced after recall compared with the memory phase (Fig. 2C, 2D). In all animals, the vast majority of reads consisted of up to three highly expanded clones. In this phase of the response, no significant dif-

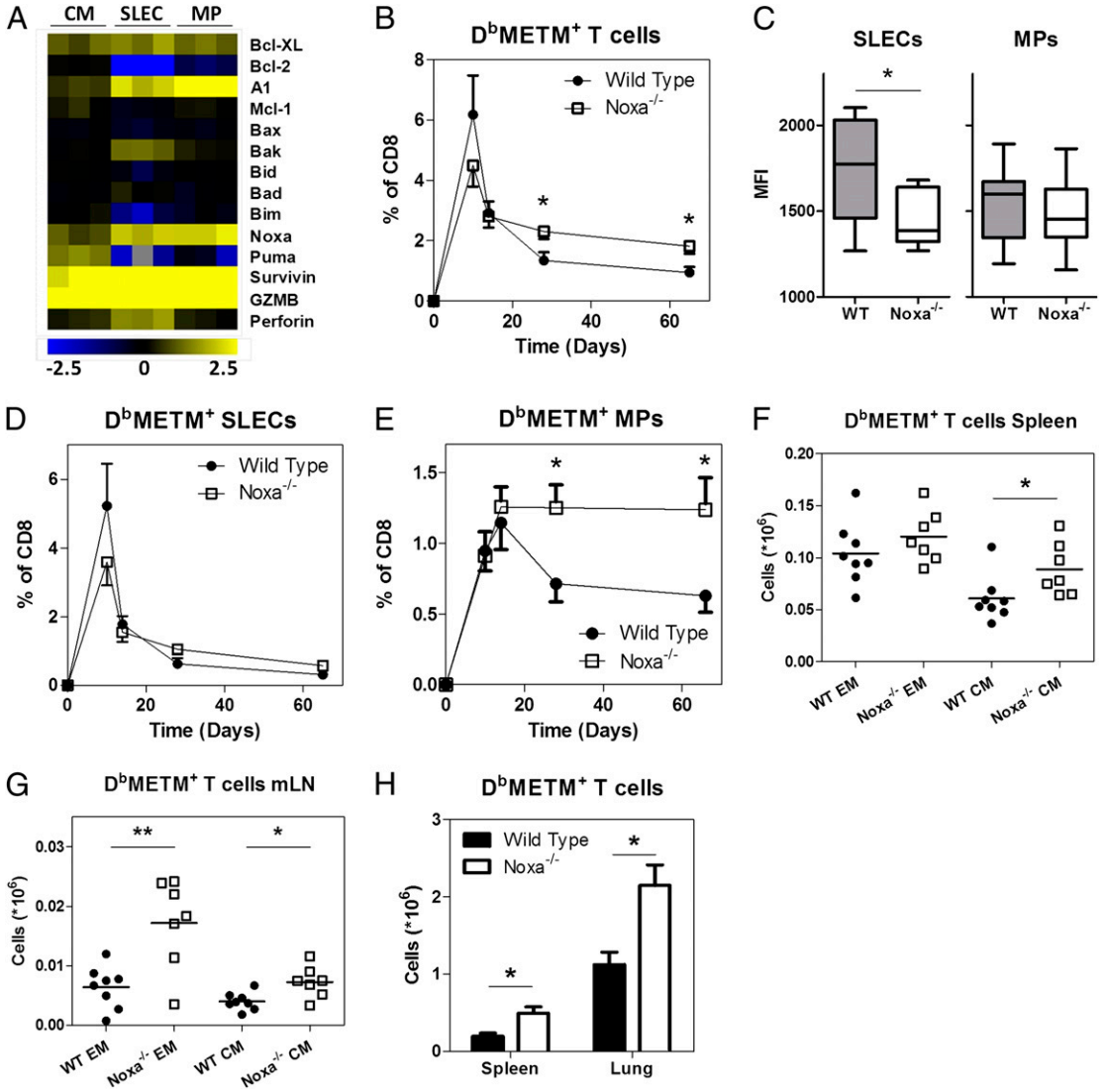

FIGURE 1. Noxa limits the number of CD8$^+$ memory T cells. (**A**) Naive (CD3$^+$CD4$^-$CD8$^+$CD44^{dim}CD62L$^+$), central memory (CD3$^+$CD4$^-$CD8$^+$CD44^{bright}CD62L$^+$), MP cells (CD3$^+$CD4$^-$C8$^+$D^{b}METM$^+$KLRG1$^-$), and SLECs (CD3$^+$CD4$^-$CD8$^+$D^{b}METM$^+$KLRG1$^+$) were sorted to >99% purity from splenocytes of mice infected 10 d previously with influenza PR8. mRNA expression of proapoptotic and antiapoptotic regulators was analyzed by RT-MLPA. Differential gene expression is represented in a heat map after log transformation of expression levels (scale is from −2.5 to 2.5), relative to averaged values of naive cells at day 0 (n = 3). Granzyme B (GZMB) expression values for naive cells were below detection levels. For calculations, these were set at an arbitrary lower threshold value of 0.02 per group. Notably, GZMB levels were 11- (±3,5) and 81-fold (±26) higher in SLECs than in MP and CM cells, respectively. (**B**–**E**) Mice were infected with influenza virus HKx31, and Ag-specific T cell responses were followed over time in the blood. (B) Relative number of D^{b}METM$^+$ cells as a percentage of CD8 T cells. (C) Quantification of the MFI of D^{b}METM$^+$ SLEC (CD8$^+$D^{b}METMCD127$^-$KLRG1$^+$; *left panel*) and MP (CD8$^+$D^{b}METM$^+$CD127$^+$KLRG1$^-$; *right panel*) cells 8 d postinfection. (D) Relative number of D^{b}METM$^+$ SLECs as a percentage of CD8 T cells. (E) Relative number of D^{b}METM$^+$ MP cells as a percentage of CD8 T cells. (**F** and **G**) Mice were infected with influenza PR8, and 84 d postinfection, Ag-specific cells were analyzed. Absolute numbers of Ag-specific memory cells in (F) spleen and (G) mediastinal LNs. (**H**) Mice were infected with influenza HKx31 and reinfected with PR8 after 66 d (n = 8 per genotype). Absolute numbers of D^{b}METM$^+$ CD8 T cells in the spleen and lungs of mice, 8 d after reinfection. *$p < 0.05$, **$p < 0.005$ (Student t test). CM, central memory (CD8$^+$D^{b}METM$^+$CD44^{bright}CD62L$^+$); EM, effector memory (CD8$^+$D^{b}METM$^+$CD44$^+$CD62L$^-$).

ferences in clonal frequency were observed between WT and Noxa$^{-/-}$ animals (Fig. 2D).

Our data show that Noxa is redundant for selection of T cell clones from the memory pool during reinfection with a pathogen bearing the same epitope. This is in contrast with its important role in selection of naive cells into the effector and, to a lesser extent, into the memory repertoire (15). However, increased clonal diversity of the memory cell pool could not completely explain the increased number of memory cells in Noxa$^{-/-}$ mice, suggesting that Noxa has a role beyond affinity-based selection.

Noxa ablation has a minor effect on the quality of memory and recall responses

The increased diversity of the memory cell repertoire of Noxa$^{-/-}$ mice prompted us to investigate whether the quality of memory cells was affected in these animals. Previously, we have shown that Noxa expression exerts selective pressure on the flu-specific CD8 T cell population to enhance the affinity of the primary effector response (15). Surprisingly, the MFI of tetramer binding was not different between flu-specific memory cells of WT and Noxa$^{-/-}$ mice (Fig. 3A). To test Noxa-deficient memory cells in

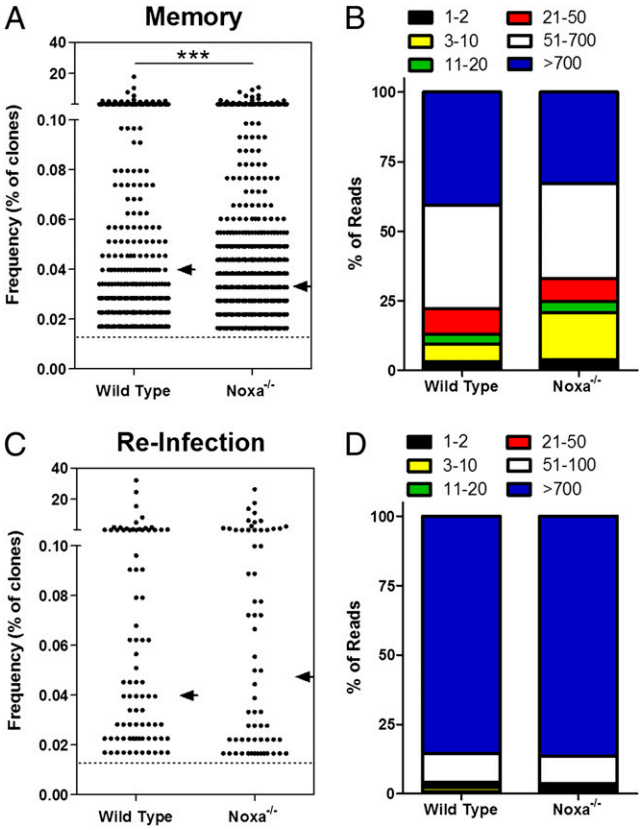

FIGURE 2. After influenza infection, Noxa$^{-/-}$ mice show higher numbers of marginally expanded clones in the CD8$^+$ memory T cell compartment. (**A** and **B**) D^{b}METM$^+$ CD8 T cells were sorted to >99% purity 84 d after influenza PR8 infection, and Vβ8.3 gene fragments were analyzed by deep sequencing. On average, 6194 reads (±409) were analyzed per mouse (WT: $n = 3$, Noxa$^{-/-}$: $n = 3$). (A) Frequency of individual clones as a percentage of total reads per genotype. Percentages were used to compensate for differences in clones sequenced per mouse. Shown are pooled data from three mice per genotype. Clones that were retrieved only one to two times (below the dotted line) were excluded from this analysis to prevent "pollution" by naive cells. Arrows indicate medians. (B) Clones were divided in six categories, based on the frequency with which they were retrieved (1–2 times, 3–10 times, 11–20 times, 21–50 times, 51–700 times, or >700 times). Relative contribution of each of these categories to the total number of reads is given. (**C** and **D**) D^{b}METM$^+$ CD8 T cells were sorted to >99% purity, 9 d after secondary infection with influenza PR8, 65 d after primary infection with influenza HKx31. Vβ8.3 gene fragments were analyzed by deep sequencing. On average, 5954 reads (±381) were analyzed per mouse (WT: $n = 3$, Noxa$^{-/-}$: $n = 3$). (C) Frequency of individual clones as a percentage of total reads per genotype. Percentages were used to compensate for differences in clones sequenced per mouse. Shown are pooled data from three mice per genotype. Clones that were retrieved only one to two times (below the dotted line) were excluded from this analysis to prevent "pollution" by naive cells. Arrows indicate medians. (D) Clones were divided in six categories as in (B). Relative contribution of each of these categories to the total number of reads is given. ***$p < 0.0001$ (Mann–Whitney U test).

a functional assay, we restimulated splenocytes of WT and Noxa$^{-/-}$ mice, infected 84 d previously, in vitro with limiting concentrations of viral peptides and analyzed IFN-γ production. We observed that Noxa$^{-/-}$ memory T cells were similarly (SSLENFRAYV) or only slightly less (ASNENMETM) responsive to decreasing doses of Ag (Fig. 3B). This suggests that Noxa only modestly increases the affinity of memory T cells. This is in accordance with the notion that, even though the Ag-specific memory population of Noxa$^{-/-}$ mice contained two times more clones, these cells represented only ~10% of the total number of tetramer-binding memory cells (Fig. 2B). Apparently, this number is too small to have a measurable impact on the peptide responsiveness of the memory cell pool as a whole. To test the capacity of Noxa-deficient memory T cells to clear infected cells, an in vivo cytotoxicity assay was performed. Splenocytes of naive congenic mice (CD45.1) were pulsed with the viral peptides ASNENMETM, SSLENFRAYV, and LSLRNPILV to mimic viral infection, or with the control OVA peptide SIINFEKL. Pulsed cells were differentially labeled with DDAO, CFSE, or both and injected in WT and Noxa$^{-/-}$ mice (CD45.2) that had been infected with influenza virus 50 d previously. ASNENMETM and SSLENFRAYV pulsed cells were cleared very efficiently, which corresponds with their previously reported immunodominance in antiviral CD8 T cell responses (31). Clearance of pulsed cells was not reduced and even slightly increased in Noxa$^{-/-}$ mice (Fig. 3C). Together, our data indicate that after influenza infection, Noxa$^{-/-}$ mice form increased memory cell numbers. These cells are of sufficient affinity to generate a comparable response as memory cells of WT mice.

Subsequently, the quality of the recall response was investigated. Mice were infected with HKx31, and after 2 mo reinfected with PR8 and analyzed 8 d later. In accordance with the increased number of D^{b}METM binding cells, compared with WT mice, Noxa$^{-/-}$ animals showed significantly higher numbers of CD8$^+$ T cells producing IFN-γ after in vitro restimulation with ASNENMETM peptides (Fig. 3D). Next, the Ag affinity of these cells was assessed. During acute infection, significantly reduced D^{b}METM staining was found for Noxa-deficient T cells after influenza infection (Fig. 3E, *top panels*). However, when the MFI of T cells was analyzed at the peak of the recall response, this difference between WT and Noxa-deficient mice was no longer observed (Fig. 3E, *bottom panels*). Restimulation with limiting concentrations of viral peptides and analysis of IFN-γ responses did not reveal differences in Ag responsiveness between secondary effector cells of WT and Noxa$^{-/-}$ mice (Fig. 3F). The equal left-shift (and thus enhanced affinity) of the WT and Noxa$^{-/-}$ curves compared with those of the primary response (Fig. 3B, *bottom panel*) is in accordance with similar narrowing of the Ag-specific repertoire during recall (Fig. 3C, 3D).

These findings indicate that affinity-based selection of long-term memory CD8 T cell clones is not as strongly dependent on Noxa as selection of primary effector cells. Moreover, Noxa does not have an essential role in affinity-based selection of secondary effector cells during homologous recall responses.

Noxa enhances cross-reactive CD8 T cell responses

We questioned whether the role of Noxa in clonal selection during recall responses was not observed, because we used a model in which dominant clones preferentially expand from a memory repertoire that is preselected on the same epitope. To increase interclonal competition between memory cells, we therefore set up a cross response, in which memory cells respond to an epitope they have not encountered previously (3).

WT and Noxa$^{-/-}$ mice were infected with influenza PR8 virus, and reinfected with the heterologous influenza virus HK2/68. The latter virus contains the immunodominant epitope ASNENMDAM that is distinct from ASNENMETM, the immunodominant epitope of PR8. Infection with one virus generates memory cells of which a minor fraction is able to recognize both epitopes. Low-frequency clones from this population generate the cross-reactive response upon reinfection with the other virus (3). The presence of cross-reactive cells was investigated using tetramers for both epitopes

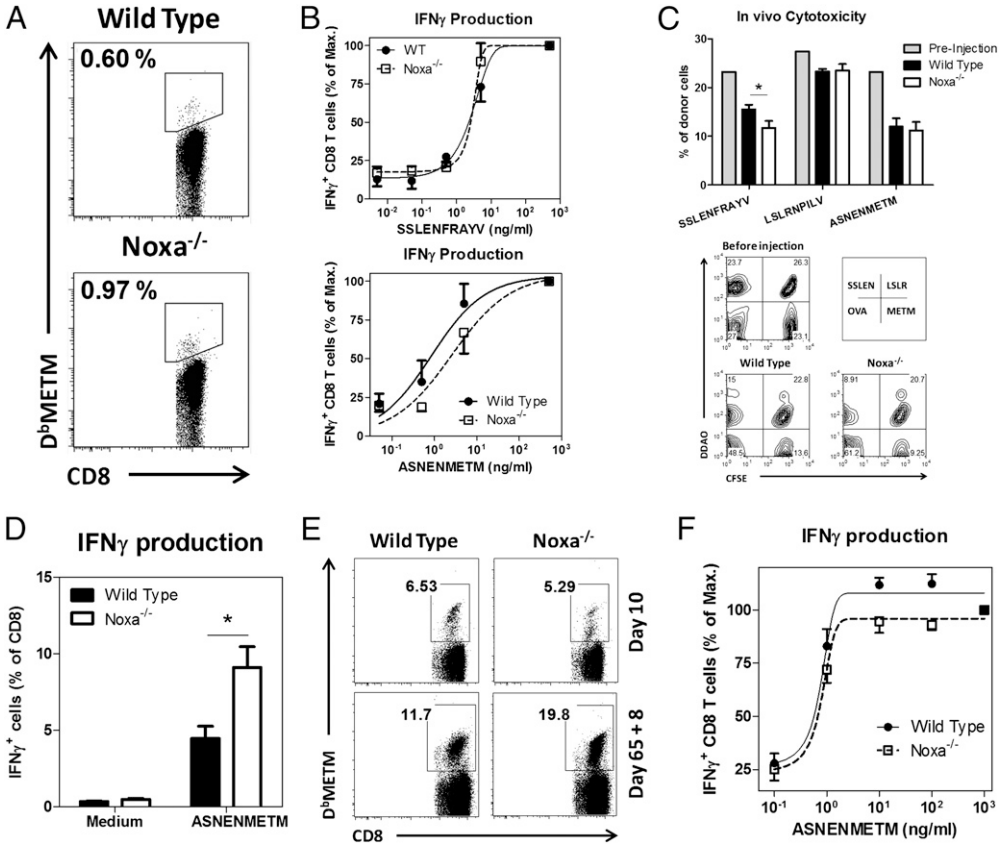

FIGURE 3. Noxa ablation has a minor effect on the quality of memory and recall responses. (**A** and **B**) Mice were infected with influenza PR8 and 84 d postinfection, Ag-specific cells were analyzed. (A) Representative FACS plots of splenic D^bMETM-specific CD8 T cells. Gated is for $CD8^+CD127^+$ cells. (B) IFN-γ production induced by varying doses of peptide in (*top panel*) SSLENFRAYV and (*bottom panel*) ASNENMETM restimulated $CD8^+$ T cells, relative to the level of cells stimulated with saturating (500 ng/ml) peptide. (**C**) WT or $Noxa^{-/-}$ mice (CD45.2) were infected with influenza PR8. Fifty days postinfection, splenocytes from naive mice (CD45.1) were fluorescently labeled, pulsed with the viral peptides ASNENMETM (METM), SSLENFRAYV (SSLEN), LSLRNPILV (LSLR), or the control peptide SIINFEKL (OVA). Cells were injected in infected recipients, and clearance of viral peptide-pulsed cells was measured after 18 h in the blood. (*top panel*) Fraction of pulsed cells as a percentage of total donor cells. (*bottom panel*) Representative FACS plots of $CD45.1^+$ cells before and 18 h after injection. (**D**–**F**) Mice were infected with influenza PR8 and reinfected with influenza HKx31 after 65 d ($n = 8$ per genotype). (D) Relative number of IFN-γ–producing cells after in vitro restimulation with ASNENMETM peptides. (E) Representative FACS plots of CD8 T cells stained with D^bMETM (first infection) 10 d postinfection with influenza HKx31 or (second infection) 8 d after reinfection with influenza PR8. Gated is for $CD8^+$ cells. (F) IFN-γ production induced by varying doses of peptide in ASNENMETM restimulated $CD8^+$ T cells, relative to the level of cells stimulated with saturating (500 ng/ml) peptide. $*p < 0.05$ (Student *t* test).

(D^bMETM and D^bMDAM) with different fluorescent labels. As observed previously (15), upon primary infection, $Noxa^{-/-}$ mice generated reduced numbers of D^bMETM^+ cells, which were also of decreased affinity (Fig. 4A, 4B). In contrast, no differences were observed in the number of cross-reactive cells between WT and $Noxa^{-/-}$ mice (Fig. 4C). When binding affinities were compared between D^bMETM^+ subsets, Noxa-deficient $D^bMETM^+D^bMDAM^-$ single-positive cells bound D^bMETM with significantly reduced intensity. $D^bMETM^+D^bMDAM^+$ double-positive cells of these mice bound both tetramers with equal intensity as WT cross-reactive cells (Fig. 4D, 4E).

When cross-reactive memory populations were compared on day 60 postinfection, a small increase of cross-reactive cells as a fraction of total Ag-specific cells was observed in $Noxa^{-/-}$ mice, but this difference was not significant (Fig. 4F). Also, affinity differences were observed in $D^bMETM^+D^bMDAM^-$ cells, but not in $D^bMETM^+D^bMDAM^+$ cells (Fig. 4G, 4H). Markedly, in contrast with recall responses against the same epitope, reinfection with the cross-reactive virus resulted in significantly reduced effector cell numbers in Noxa-deficient mice compared with WT mice (Fig. 4I, 4J). Thus, similar to naive cells, memory cells require Noxa for selection into effector responses if the precursor frequency of high-affinity cells is low.

Noxa controls memory T cell formation and not T cell contraction

Next to the effect of Noxa on the quality of the memory response, Noxa also limited the size of the total memory population. The increased memory formation observed in $Noxa^{-/-}$ mice may have resulted from delayed T cell contraction after antigenic clearance. Contraction can be investigated by following the survival of flu-specific cells after adoptive transfer into pathogen-free animals. WT and $Noxa^{-/-}$ mice (CD45.1) were infected with PR8 virus and 10 d postinfection, total splenic CD8 T cells were isolated and equal numbers of cells were injected into congenic (CD45.2) naive hosts (Fig. 5A). Because of the abrupt lack of an inflammatory environment for the transferred virus-specific cells, direct contraction of the Ag-specific pool ensues under these conditions (32). Ag-specific donor T cells could be observed up to day 28, after which their numbers declined below detection levels. During this period, no difference was observed in the contraction of Ag-specific cells between WT and $Noxa^{-/-}$ cells (Fig. 5B). This

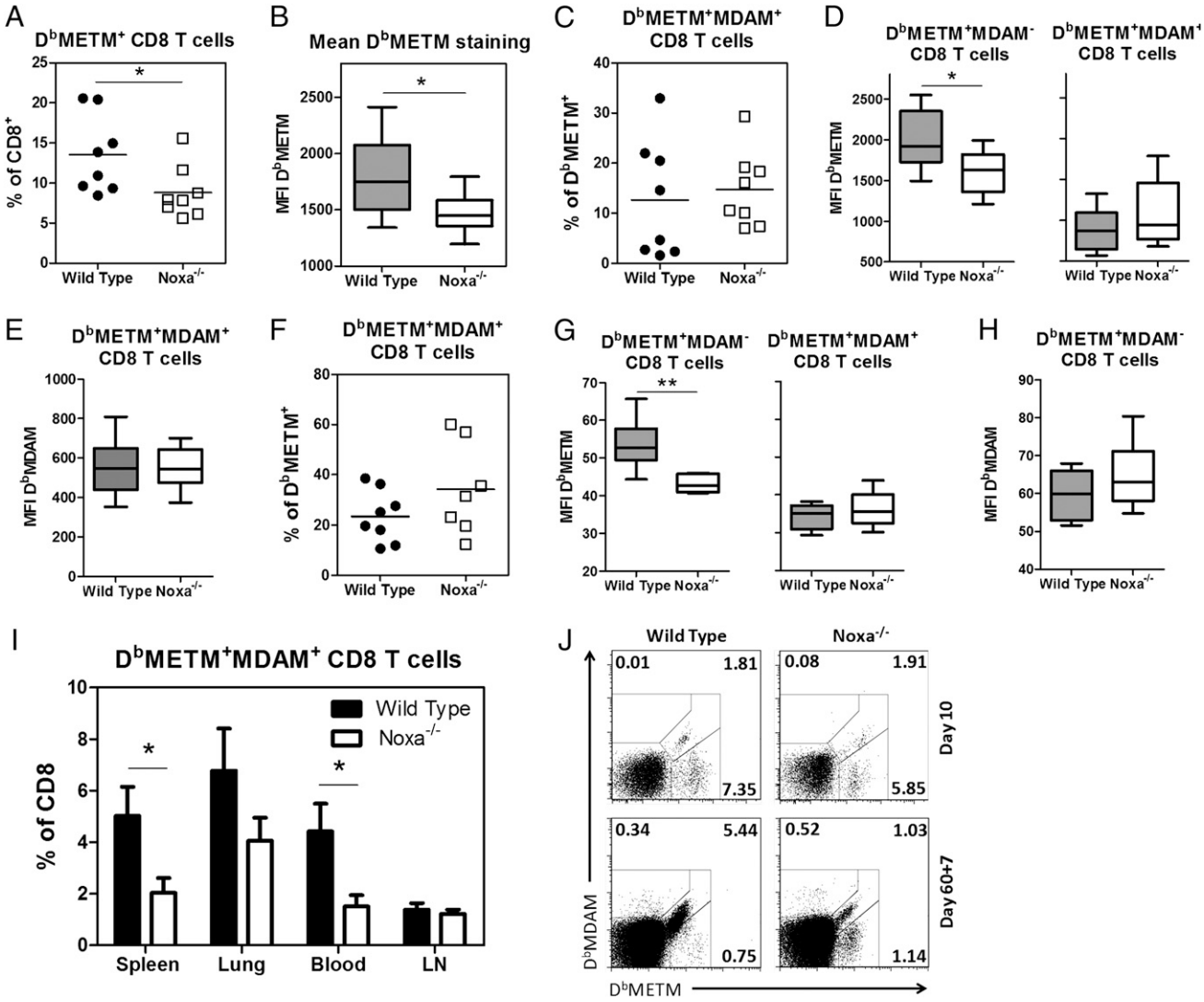

FIGURE 4. Noxa ablation reduces cross-reactive memory responses. Mice were infected with the ASNENMETM-epitope expressing influenza strain PR8. Sixty days after primary infection, mice were reinfected with the ASNENMDAM-epitope expressing influenza strain HK2/68. Seven days after secondary infection, mice were sacrificed and organs analyzed. (**A**–**E**) Analysis of Ag-specific cells 10 d after primary infection. (A) Number of D^bMETM^+ cells in the blood of infected mice, as a percentage of CD8 T cells. (B) Quantification of the intensity of D^bMETM staining within the D^bMETM^+ CD8 T cell pool. (C) Number of cross-reactive ($D^bMETM^+D^bMDAM^+$) cells as a percentage of D^bMETM^+ CD8 T cells. (D) Quantification of the intensity of D^b METM staining within the $D^bMETM^+D^bMDAM^-$ (*left panel*) and $D^bMETM^+D^bMDAM^+$ (*right panel*) CD8 T cell populations. (E) Quantification of the intensity of D^bMDAM staining within the $D^bMETM^+D^bMDAM^+$ CD8 T cell population. (**F**–**H**) Analysis of Ag-specific cells 60 d after primary infection. (F) Number of cross-reactive ($D^bMETM^+D^bMDAM^+$) cells as a percentage of D^bMETM^+ CD8 T cells. (G) Quantification of the intensity of D^bMETM staining within the $D^bMETM^+D^bMDAM^-$ (*left panel*) and $D^bMETM^+D^bMDAM^+$ (*right panel*) CD8 T cell populations. (H) Quantification of the intensity of D^bMDAM staining within the $D^bMETM^+D^bMDAM^+$ CD8 T cell population. (**I** and **J**) Analysis of Ag-specific cells 7 d after secondary infection. (I) Relative number of cross-reactive ($D^bMETM^+D^bMDAM^+$) cells as a percentage of CD8 T cells in the indicated organs. (J) Representative FACS plots of peripheral blood CD8 T cells stained with tetramers. Gated is for $CD8^+$ cells. $*p < 0.05$, $**p < 0.005$ (Student *t* test).

argues against a role for Noxa in the contraction phase of the antiviral response, which underlines previous findings after HSV infection (33).

In the PR8-HKx31 influenza infection model, the relative increase of Ag-specific cell numbers was identical between WT and Noxa-deficient mice during the recall response (Fig. 1F). If increased memory cell numbers are formed in $Noxa^{-/-}$ mice during priming, infection of recipient mice should result in increased Noxa-deficient donor cell numbers in the earlier mentioned adoptive transfer model. Therefore, 1 mo after transfer, recipient mice were infected with PR8 virus. Noxa-deficient memory T cells expanded significantly more than transferred WT cells both in relative and absolute numbers. This effect was more pronounced in the lungs, the site of viral replication, than in spleen, blood, and LNs (Fig. 5C–E).

Together, these data show that Noxa plays a role in controlling the number of memory cells that is formed early postinfection, but does not affect contraction.

Noxa ablation leads to increased memory inflation during chronic mCMV infection

In humans, boosting of the CD8 memory T cell pool is most pronounced postinfection with chronic viruses such as CMV. CMV causes a chronic, latent infection that is never cleared. After the acute phase upon primary infection, CMV remains latently present in its host, but is regularly reactivated, which causes flares of the

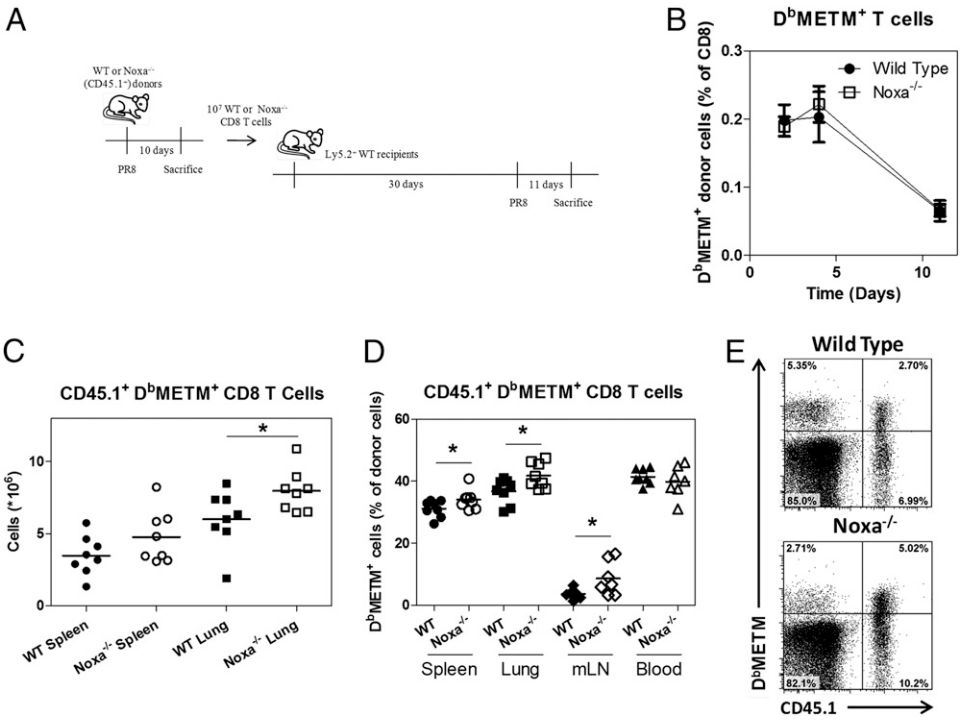

FIGURE 5. Enhanced recall responses of Noxa$^{-/-}$ CD8 T cells results from increased formation of memory cells early during the immune response. WT and Noxa$^{-/-}$ mice (CD45.1) were infected with influenza PR8. Ten days later, total CD8 T cells were isolated and injected in naive WT recipients (CD45.2). Thirty days after injection, recipient mice were infected with influenza PR8 (n = 8 per genotype). (**A**) Schematic representation of the experimental setup to determine whether Noxa limits memory CD8 T cell precursor numbers during the priming phase of influenza infection. (**B**) Donor D^{b}METM$^+$ CD8 T cells in the blood of recipient mice, as a percentage of CD8 T cells. (**C** and **D**) Donor D^{b}METM$^+$ CD8 T cells (C) in absolute numbers and (D) as a percentage of donor CD8 T cells. (**E**) Representative FACS plots of spleen cells shown in (C). Gated is for CD8$^+$ T cells. *$p < 0.05$ (Student t test).

antiviral response (34). This continuous boost of the immune system results in a gradual increase of CMV-specific CD8 T cells, a so-called memory inflation, which will ultimately comprise a very significant percentage of the total CD8 T cell pool both in humans and in mice (34).

To investigate the role of Noxa in this model of chronic infection, we studied WT and Noxa$^{-/-}$ mice infected with mCMV and CD8 T cell responses directed against three different viral H2K^b epitopes: one epitope that only induces a CD8 response during the acute phase of mCMV infection (m57$_{816–824}$), one epitope that is only immunodominant during memory inflation (IE3/m122$_{416–475}$), and one epitope that is present during both responses (m139$_{416–423}$) (35).

As reported previously 10 d postinfection with influenza virus, mCMV infection did not result in a different number of CD8 T cells with an effector phenotype (CD44$^+$CD62L$^-$) during the peak of the antiviral response (15). When Ag-specific cell numbers were quantified, modestly reduced numbers of CD8$^+$ T cells directed against m57 and m139 were observed in Noxa$^{-/-}$ compared with WT mice (Fig. 6A and data not shown). As expected, no T cell response against IE3 was observed during acute infection. When the intensity of tetramer staining was assessed, a clear reduction in tetramer binding was observed in Noxa$^{-/-}$ mice for the m57$_{816–824}$ and m139$_{416–423}$ epitopes (Fig. 6B, 6C). When splenic T cells were restimulated in vitro on day 8 postinfection, a clearly reduced affinity for the m57$_{816–824}$ peptide also was observed (Fig. 6D). As reported previously (15), no differences were observed in expression levels of CD3 or TCRβ in Noxa$^{-/-}$ effector cells compared with WT cells, excluding enhanced TCR downregulation as a cause of reduced tetramer staining (data not shown). Together, these data indicate that, identical to influenza infection, also during primary mCMV infection, Noxa-deficient mice generate an effector T cell response of reduced affinity.

Subsequently, antiviral CD8 T cell formation was analyzed during the chronic phase of mCMV infection, 4 mo postinfection. In most analyzed organs, an increase in the absolute number of CD8 T cells was observed in Noxa$^{-/-}$ mice (Fig. 7A). Phenotypic analysis of these cells revealed an increase of both effector and memory cells in these organs (Fig. 7B and data not shown). When Ag-specific cells were investigated, in particular the inflationary T cell pool directed against IE3$_{416–475}$ was enlarged (Fig. 7C). However, also the noninflationary m57$_{816–824}$–specific pool, which primarily had a memory cell phenotype (data not shown), was increased in cell numbers. This corresponds with the observation that Noxa-deficient mice have increased numbers of memory cells after acute influenza infection. In contrast, the m139$_{416–423}$–specific pool was not significantly increased.

Together, these data indicate that repetitive boosting of the Ag-specific CD8 T cell pool during chronic mCMV infection causes enhanced memory cell inflation in Noxa$^{-/-}$ mice.

Persistent activation of the T cell compartment leads to lethal pathology in Noxa$^{-/-}$ mice

mCMV infection represents a model in which the CD8 T cell compartment is continuously triggered by low doses of Ag. Other infections, such as HIV infection in humans, lead to a constant activation of the immune system because of the continuous presence of high viral titers. Next, we investigated T cell responses in Noxa$^{-/-}$ mice under conditions of persistent immune activation. For this purpose, a transgenic mouse model was used. Costimulation via CD70 and CD27 directs differentiation of naive T cells into effectors (36). CD70^{TG} mice possess an enlarged fraction of effector T cells, which is driven by hyperresponsiveness to environmental Ag. These animals display signs of chronic immune activation, strikingly resembling HIV infection (37, 38). Therefore, Noxa$^{-/-}$ mice were crossed with CD70^{TG} mice.

Under homeostatic conditions, CD70^{TG} mice remain relatively healthy for at least 6–8 mo but eventually die of opportunistic infections as a result of T cell depletion (38). In stark contrast with this gradual phenotype, Noxa$^{-/-}$xCD70^{TG} (Noxa70) mice displayed severe organ pathology, including splenomegaly, lung damage, and liver fibrosis at an early age (Fig. 8A and data not

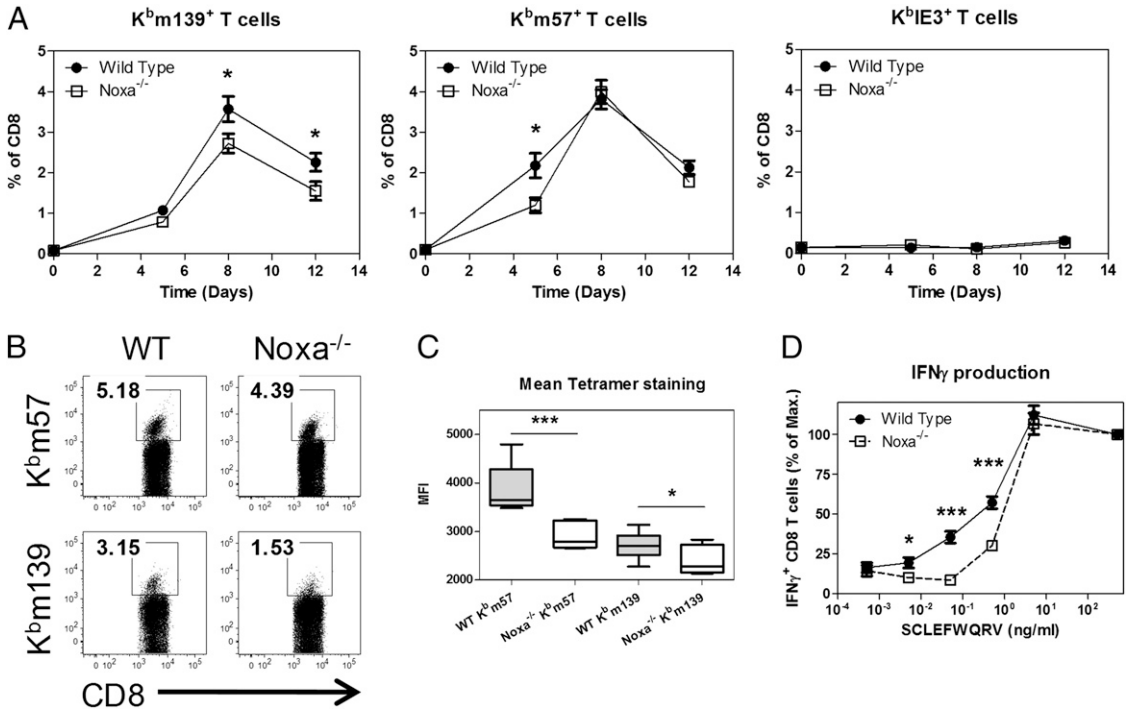

FIGURE 6. Acute mCMV infection of Noxa$^{-/-}$ mice leads to the formation of effector cells of reduced Ag affinity. (**A**–**D**) Mice were infected i.p. with 5×10^5 PFU mCMV, and Ag-specific responses were followed for three viral epitopes. Shown is one of three experiments ($n = 8$). (A) Number of (*left panel*) K^{b}m139$^+$, (*middle panel*) K^{b}m57$^+$, and (*right panel*) K^{b}IE3$^+$ CD8 T cells, as a percentage of CD8 T cells. (B) Representative FACS plots of tetramer-stained CD8 T cells 8 d postinfection. Gated is for CD8 T cells. (C) Quantification of the MFI of D^{b}m57$^+$ cells 8 d postinfection. (D) IFN-γ production induced by varying doses of peptide in SCLEFWQRV restimulated CD8 T cells, relative to the level of cells stimulated with saturating (500 ng/ml) peptide. $*p < 0.05$, $***p < 0.0005$ (Student t test).

shown). Pathology culminated in premature death with a median survival of only 16 wk (Fig. 8B). In contrast with CD70^{TG} mice, organ damage in Noxa70 mice was associated with accumulation of T cells in spleen, liver, and lung, of which a large fraction had an SLEC phenotype (Fig. 8C, 8D, and data not shown). Activated caspase-3 staining in the spleen showed less apoptotic cells in Noxa70 mice, indicating that the accumulation of lymphocytes was the result of decreased apoptosis compared with CD70^{TG}

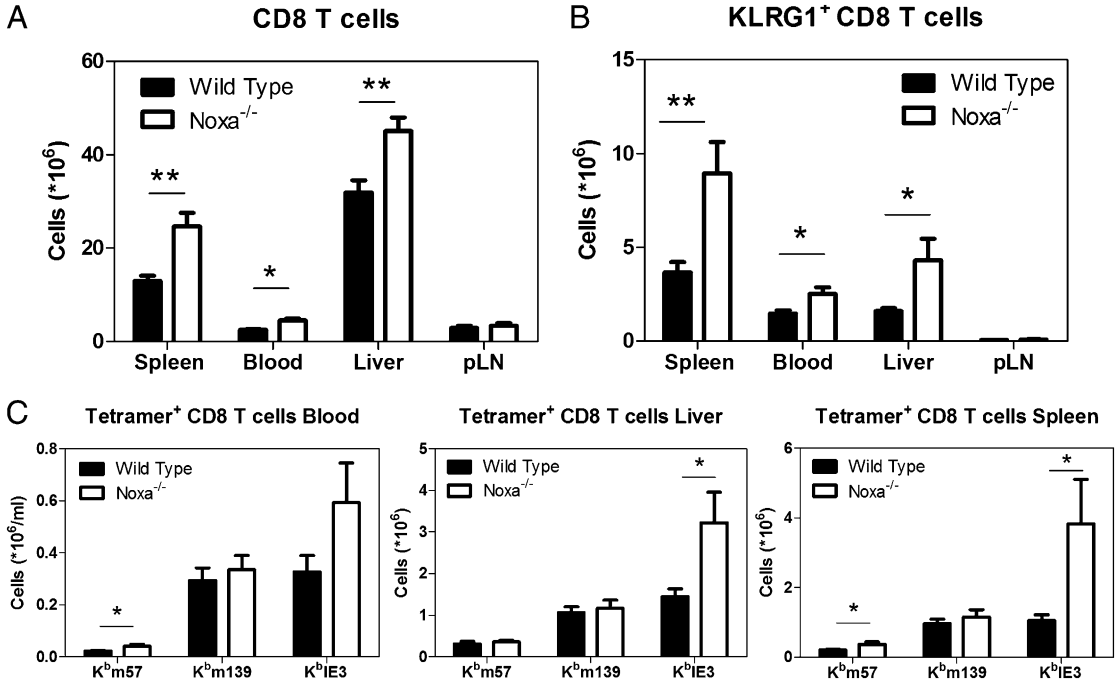

FIGURE 7. Noxa$^{-/-}$ mice have increased memory inflation during chronic mCMV infection. Mice were infected i.p. with 5×10^5 PFU mCMV, and Ag-specific responses were analyzed 140 d later. Shown is one of two experiments ($n = 8$). (**A**) Total number of CD8 T cells in various organs of infected mice. (**B**) Total effector CD8 T cell numbers (KLRG1$^+$) in organs of infected mice. (**C**) Total number of Ag-specific CD8 T cells in various organs of infected mice. $*p < 0.05$, $**p < 0.005$ (Student t test).

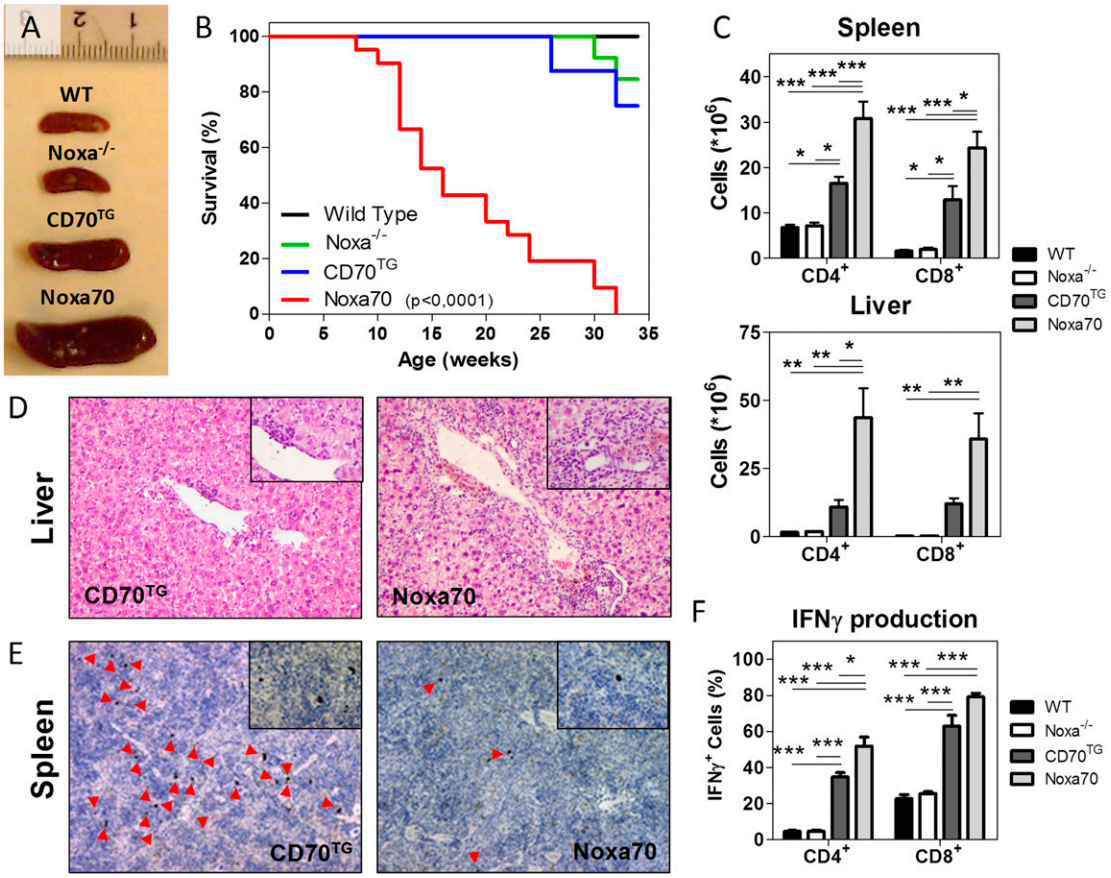

FIGURE 8. Noxa ablation during persistent T cell activation culminates in lethal pathology. (**A**) Representative spleens of WT, Noxa$^{-/-}$, CD70^{TG}, and Noxa70 mice at 12 wk of age. (**B**) Kaplan–Meier survival plot for mice of indicated genotypes housed under specific pathogen-free conditions. WT (n = 8), Noxa$^{-/-}$ (n = 12), CD70^{TG} (n = 7), Noxa70 (n = 21). (**C**) Effector/effector memory cell (CD44^{+}CD62L^{-}) numbers in spleen and liver of WT, Noxa$^{-/-}$, CD70^{TG}, and Noxa70 mice at 12 wk of age (n = 4–7). (**D**) H&E analysis of liver sections (original magnification ×10, *inset* ×40) from CD70^{TG} and Noxa70 mice at 15 wk of age, showing increased leukocyte infiltrates in Noxa70 compared with CD70^{TG} mice. (**E**) Activated caspase-3 and hematoxylin staining in spleen sections (original magnification ×10, *inset* ×40) of mice at 15 wk of age, showing reduced numbers of apoptotic cells (marked by arrowheads) in Noxa70 compared with CD70^{TG} mice. (**F**) Cytokine production of CD4 and CD8 T cells from the spleens of WT, Noxa$^{-/-}$, CD70^{TG}, and Noxa70 mice, stimulated with PMA/ionomycin in the presence of brefeldin A. Number of IFN-γ–producing cells as a percentage of the total CD4 or CD8 T cell pool is given. *$p < 0.05$, **$p < 0.005$, ***$p < 0.0005$ (Mantel–Cox and one-way ANOVA tests).

mice (Fig. 8E). As reported previously (38), CD70^{TG} CD4 and CD8 T cells produce high levels of IFN-γ upon in vitro restimulation. This phenotype was aggravated in absence of Noxa (Fig. 8F). Together, these data show that Noxa prevents leukocyte-mediated organ pathology under conditions of chronic immune activation.

Discussion

Upon activation, both effector and MP cell populations are subject to control mechanisms that determine their appropriate magnitude and diversity. In this article, we have shown that, in addition to controlling formation of the effector T cell pool (15), the proapoptotic BH3-only member Noxa is a mediator of memory cell formation. Its ablation resulted in an increase of the overall size and diversity of the antiviral memory T cell pool. This implies that Noxa normally mediates elimination of MP cells that have expanded beyond the amount that can be sustained by their environment. Loss of Noxa was not beneficial for overall immunity because it impaired cross-reactivity and resulted in severe immunopathology under conditions of chronic immune activation.

An open question is whether the role of Noxa during effector and memory T cell formation comprises two different mechanisms or represents two aspects of the same apoptotic checkpoint. Previously we showed that the Noxa/Mcl-1 axis mediates affinity-based T cell selection dependent on IL-2R–mediated control of Mcl-1 stability. MP T cells also express the IL-2R (39, 40). However, IL-15 appears to play a more prominent role in the formation and maintenance of memory cells (41). Others have shown that Noxa plays a role in the induction of NK cell apoptosis upon IL-15 deprivation (42). Thus, Noxa may also mediate IL-15–dependent survival of MP T cells early during the immune response.

In line with this hypothesis, we present Noxa as a regulator of activated T cell survival, specifically acting during the initial phase of primary expansion. The physiological effects of its induction will depend on the context; Noxa is induced upon TCR triggering and, unlike the potent BH3-only proteins Bim and Puma, its levels are not highly dependent on the availability of costimulation or cytokines (9, 15). We summarize the various effects of Noxa on T cell responses in the following model (Fig. 9): under conditions of stringent selection, such as during effector cell formation upon acute infection, the effects of Bim and Puma are dominant (15, 33, 43), causing only increased diversity of the effector pool in absence of Noxa (Fig. 9A). Memory cell formation is subject to less stringent selection criteria, and the memory cell pool therefore has increased clonal diversity compared with the effector cell pool, also under Noxa-sufficient conditions (24). During this phase,

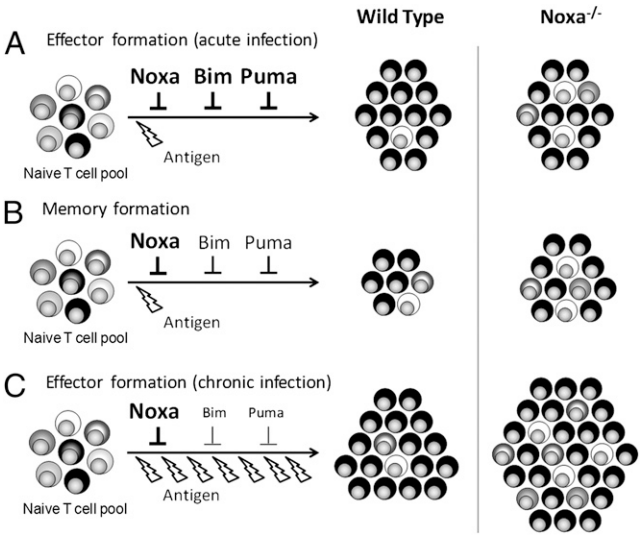

FIGURE 9. Model of the context-dependent effects of Noxa on T cell expansion. Noxa expression is induced by TCR triggering, and its selective pressure on activated T cell populations will be similar in different situations. However, because of changing contributions of Bim and Puma, Noxa ablation has different consequences. (**A**) During effector cell formation upon acute infection, available nutrients and cytokines are restricted, and redundancy between the BH3-only proteins Noxa, Bim, and Puma prevents excessive T cell expansion. Absence of Noxa only results in enhanced diversity of the effector pool. (**B**) Selection of activated T cells into the memory cell pool is less stringent, allowing more clones to contribute to this population. Because of reduced pressure from other BH3-only molecules, absence of Noxa results both in a larger and more diverse memory population. (**C**) In the continuous presence of Ag, expansion is even less restricted, resulting in a greatly increased number of effector cells. Absence of Noxa results in enhanced expansion of all cells. Note that colors of cells denote different clones.

there is less redundancy of BH3-only members and Noxa ablation results in both increased size and diversity of the memory cell pool (Fig. 9B) (15, 33, 43). In the case of chronic immune activation, ample Ag, costimulation, and cytokines are available for activated T cells, and the role of Bim and Puma in the control of cell numbers will be even more reduced. In this situation, Noxa has a dominant role in limiting T cell expansion, and its ablation results in lethal pathology (Fig. 9C).

From a clinical point of view, our findings may be of interest. An important goal of new vaccine strategies is to alter the broadness and size of the immune response (44). A standing question is therefore whether optimal size and diversity is already inherently present in the immune system, or whether altered selective pressure on memory cell formation may further enhance or cripple T cell recall responses. Reducing Noxa-mediated apoptosis during priming appeared as a promising target to enhance memory responses. Indeed, ablation of Noxa resulted in a larger and more diverse memory cell population, and in enhanced T cell expansion upon reinfection with a similar pathogen.

Interestingly, despite this increased diversity, Noxa$^{-/-}$ mice mounted a reduced cross-reactive T cell response. This is unexpected, as a more diverse memory cell population statistically has a higher chance of having a high-affinity clone against an altered epitope. We hypothesize that the difference between homologous and cross-reactive recall responses results from differences in selective pressure. During the homologous recall experiment, high-affinity clones in the primary response form the most dominant clones in the memory pool and subsequently the dominant clones in the secondary response (Fig. 2). During priming in the cross-reactive response, there is no selection for high-affinity clones that recognize the immunodominant epitope of the second virus. The clones that dominate the secondary response are therefore generally of very low frequency in the memory population (3). In the homologous response, re-expanding clones have a numerical advantage over other clones, and interclonal competition will therefore be of minor influence on their expansion. In the cross-reactive response, competition of low-frequency, high-affinity memory clones with each other and with naive clones will occur for limiting nutrients and cytokines (45). We envision that Noxa mediates this selection process in a similar way as in the primary response (15). This causes a reduced number of Ag-specific cells in Noxa-deficient animals during the cross-reactive response, despite the fact that, because of increased diversity of the memory cell pool, the precursor frequency of cross-reactive T cells may even be increased in these mice. However, because these experiments were performed by analyzing only a limited number of antigenic epitopes, some caution is warranted in extrapolating the results to the entire memory response. Future models, in which expression of Noxa can be regulated, must reveal whether reduction of Noxa-mediated memory cell selection is actually beneficial to cross-reactive recall responses when it only occurs during priming.

An additional finding of clinical importance is the observation that ablation of Noxa under conditions of high-grade T cell activation did not simply lead to a passive accumulation of effector memory cells, but resulted in liver and lung destruction (Fig. 8). This phenotype is distinct from other knockout mice that accumulate large numbers of lymphocytes, such as the FAS/Bim double knockout (11, 46–48). Interestingly, during acute infection models, we did not observe increased immunopathology in Noxa$^{-/-}$ mice. However, Noxa expression appeared to be highest in activated cells and went down in memory cells. In accordance with our model described earlier, this nonredundant role of Noxa in the control of effector cell numbers and function may therefore only become obvious under conditions of high or continuous antigenic pressure. Alternatively, the enhanced effector cell numbers during chronic mCMV infection and in Noxa70 mice may be the result of reactivation of increased numbers of memory cell precursors formed in the absence of Noxa.

In Noxa70 mice, we used CD27 stimulation by transgenic CD70 as a model to test whether a reduced threshold for activated T cell survival can lead to pathology. Increased CD70 expression has been well documented, however, in a variety of human diseases such as HIV infection and systemic lupus erythematosus (49). The fact that Noxa ablation induced T cell accumulation both under conditions of chronic CD27 stimulation and in a model for chronic infection with mCMV virus indicates that proper control of Ag-experienced T cell numbers by Noxa may be relevant for human disease.

In conclusion, Noxa appears to limit cell numbers both during effector and memory CD8 T cell formation. Its role in effector cell formation restricts survival of low-affinity cells, ensuring persistence of effective cells only. In the process of memory cell formation, Noxa controls memory cell numbers, whereas its effect on affinity is less pronounced. Re-encounter of Ag in Noxa$^{-/-}$ mice thus leads to enhanced effector cell formation, but lethal pathology after chronic immune activation. A proper control of apoptotic molecules therefore appears to be essential for effector and memory T cells to maintain the fine balance between too few and too many cells upon pathogen encounter and re-encounter.

Acknowledgments

We thank Andreas Strasser for providing Noxa$^{-/-}$ mice. We want to acknowledge the staff of the Academic Medical Center animal facility for excellent animal handling and care. We are grateful to Berend Hooibrink for technical assistance and thank Martijn Nolte for helpful discussions.

Disclosures

The authors have no financial conflicts of interest.

References

1. Johnson-Nauroth, J. M., J. Graber, K. Yao, S. Jacobson, and P. A. Calabresi. 2006. Memory lineage relationships in HTLV-1-specific CD8+ cytotoxic T cells. *J. Neuroimmunol.* 176: 115–124.
2. Kedzierska, K., S. J. Turner, and P. C. Doherty. 2004. Conserved T cell receptor usage in primary and recall responses to an immunodominant influenza virus nucleoprotein epitope. *Proc. Natl. Acad. Sci. USA* 101: 4942–4947.
3. van Gisbergen, K. P., P. L. Klarenbeek, N. A. Kragten, P. P. Unger, M. B. Nieuwenhuis, F. M. Wensveen, A. ten Brinke, P. P. Tak, E. Eldering, M. A. Nolte, and R. A. van Lier. 2011. The costimulatory molecule CD27 maintains clonally diverse CD8(+) T cell responses of low antigen affinity to protect against viral variants. *Immunity* 35: 97–108.
4. Pantaleo, G., J. F. Demarest, T. Schacker, M. Vaccarezza, O. J. Cohen, M. Daucher, C. Graziosi, S. S. Schnittman, T. C. Quinn, G. M. Shaw, et al. 1997. The qualitative nature of the primary immune response to HIV infection is a prognosticator of disease progression independent of the initial level of plasma viremia. *Proc. Natl. Acad. Sci. USA* 94: 254–258.
5. Edwards, B. H., A. Bansal, S. Sabbaj, J. Bakari, M. J. Mulligan, and P. A. Goepfert. 2002. Magnitude of functional CD8+ T-cell responses to the gag protein of human immunodeficiency virus type 1 correlates inversely with viral load in plasma. *J. Virol.* 76: 2298–2305.
6. Sabbagh, L., C. C. Srokowski, G. Pulle, L. M. Snell, B. J. Sedgmen, Y. Liu, E. N. Tsitsikov, and T. H. Watts. 2006. A critical role for TNF receptor-associated factor 1 and Bim down-regulation in CD8 memory T cell survival. *Proc. Natl. Acad. Sci. USA* 103: 18703–18708.
7. Wojciechowski, S., P. Tripathi, T. Bourdeau, L. Acero, H. L. Grimes, J. D. Katz, F. D. Finkelman, and D. A. Hildeman. 2007. Bim/Bcl-2 balance is critical for maintaining naive and memory T cell homeostasis. *J. Exp. Med.* 204: 1665–1675.
8. Jaleco, S., L. Swainson, V. Dardalhon, M. Burjanadze, S. Kinet, and N. Taylor. 2003. Homeostasis of naive and memory CD4+ T cells: IL-2 and IL-7 differentially regulate the balance between proliferation and Fas-mediated apoptosis. *J. Immunol.* 171: 61–68.
9. Sabbagh, L., G. Pulle, Y. Liu, E. N. Tsitsikov, and T. H. Watts. 2008. ERK-dependent Bim modulation downstream of the 4-1BB-TRAF1 signaling axis is a critical mediator of CD8 T cell survival in vivo. *J. Immunol.* 180: 8093–8101.
10. Weant, A. E., R. D. Michalek, K. E. Crump, C. Liu, A. P. Konopitski, and J. M. Grayson. 2011. Defects in apoptosis increase memory CD8+ T cells following infection of Bim$^{-/-}$Faslpr/lpr mice. *Cell. Immunol.* 271: 256–266.
11. Bouillet, P., and L. A. O'Reilly. 2009. CD95, BIM and T cell homeostasis. *Nat. Rev. Immunol.* 9: 514–519.
12. Chetoui, N., M. Boisvert, S. Gendron, and F. Aoudjit. 2010. Interleukin-7 promotes the survival of human CD4+ effector/memory T cells by up-regulating Bcl-2 proteins and activating the JAK/STAT signalling pathway. *Immunology* 130: 418–426.
13. Fox, C. J., P. S. Hammerman, and C. B. Thompson. 2005. Fuel feeds function: energy metabolism and the T-cell response. *Nat. Rev. Immunol.* 5: 844–852.
14. Fazilleau, N., L. J. McHeyzer-Williams, and M. G. McHeyzer-Williams. 2007. Local development of effector and memory T helper cells. *Curr. Opin. Immunol.* 19: 259–267.
15. Wensveen, F. M., K. P. van Gisbergen, I. A. Derks, C. Gerlach, T. N. Schumacher, R. A. van Lier, and E. Eldering. 2010. Apoptosis threshold set by Noxa and Mcl-1 after T cell activation regulates competitive selection of high-affinity clones. *Immunity* 32: 754–765.
16. Wensveen, F. M., N. L. Alves, I. A. Derks, K. A. Reedquist, and E. Eldering. 2011. Apoptosis induced by overall metabolic stress converges on the Bcl-2 family proteins Noxa and Mcl-1. *Apoptosis* 16: 708–721.
17. Hendriks, J., Y. Xiao, and J. Borst. 2003. CD27 promotes survival of activated T cells and complements CD28 in generation and establishment of the effector T cell pool. *J. Exp. Med.* 198: 1369–1380.
18. 1959. EXPERT committee on respiratory virus disease: first report. *World Health Organ. Tech. Rep. Ser.* 58: 1–59.
19. Coleman, M. T., W. R. Dowdle, H. G. Pereira, G. C. Schild, and W. K. Chang. 1968. The Hong Kong-68 influenza A2 variant. *Lancet* 2: 1384–1386.
20. Kilbourne, E. D. 1969. Future influenza vaccines and the use of genetic recombinants. *Bull. World Health Organ.* 41: 643–645.
21. van der Sluijs, K. F., L. J. van Elden, M. Nijhuis, R. Schuurman, J. M. Pater, S. Florquin, M. Goldman, H. M. Jansen, R. Lutter, and T. van der Poll. 2004. IL-10 is an important mediator of the enhanced susceptibility to pneumococcal pneumonia after influenza infection. *J. Immunol.* 172: 7603–7609.
22. Wagner, M., S. Jonjic, U. H. Koszinowski, and M. Messerle. 1999. Systematic excision of vector sequences from the BAC-cloned herpesvirus genome during virus reconstitution. *J. Virol.* 73: 7056–7060.
23. Brune, W., H. Hengel, and U. H. Koszinowski. 2001. A mouse model for cytomegalovirus infection. *Curr. Protoc. Immunol.* Chapter 19: Unit 19.7.
24. Klarenbeek, P. L., P. P. Tak, B. D. van Schaik, A. H. Zwinderman, M. E. Jakobs, Z. Zhang, A. H. van Kampen, R. A. van Lier, F. Baas, and N. de Vries. 2010. Human T-cell memory consists mainly of unexpanded clones. *Immunol. Lett.* 133: 42–48.
25. Alves, N. L., I. A. Derks, E. Berk, R. Spijker, R. A. van Lier, and E. Eldering. 2006. The Noxa/Mcl-1 axis regulates susceptibility to apoptosis under glucose limitation in dividing T cells. *Immunity* 24: 703–716.
26. Grayson, J. M., K. Murali-Krishna, J. D. Altman, and R. Ahmed. 2001. Gene expression in antigen-specific CD8+ T cells during viral infection. *J. Immunol.* 166: 795–799.
27. Verschelde, C., T. Walzer, P. Galia, M. C. Biémont, L. Quemeneur, J. P. Revillard, J. Marvel, and N. Bonnefoy-Berard. 2003. A1/Bfl-1 expression is restricted to TCR engagement in T lymphocytes. *Cell Death Differ.* 10: 1059–1067.
28. Joshi, N. S., W. Cui, A. Chandele, H. K. Lee, D. R. Urso, J. Hagman, L. Gapin, and S. M. Kaech. 2007. Inflammation directs memory precursor and short-lived effector CD8(+) T cell fates via the graded expression of T-bet transcription factor. *Immunity* 27: 281–295.
29. Flynn, K. J., G. T. Belz, J. D. Altman, R. Ahmed, D. L. Woodland, and P. C. Doherty. 1998. Virus-specific CD8+ T cells in primary and secondary influenza pneumonia. *Immunity* 8: 683–691.
30. Kedzierska, K., E. B. Day, J. Pi, S. B. Heard, P. C. Doherty, S. J. Turner, and S. Perlman. 2006. Quantification of repertoire diversity of influenza-specific epitopes with predominant public or private TCR usage. *J. Immunol.* 177: 6705–6712.
31. Thomas, P. G., S. A. Brown, R. Keating, W. Yue, M. Y. Morris, J. So, R. J. Webby, and P. C. Doherty. 2007. Hidden epitopes emerge in secondary influenza virus-specific CD8+ T cell responses. *J. Immunol.* 178: 3091–3098.
32. Sanjabi, S., M. M. Mosaheb, and R. A. Flavell. 2009. Opposing effects of TGF-beta and IL-15 cytokines control the number of short-lived effector CD8+ T cells. *Immunity* 31: 131–144.
33. Fischer, S. F., G. T. Belz, and A. Strasser. 2008. BH3-only protein Puma contributes to death of antigen-specific T cells during shutdown of an immune response to acute viral infection. *Proc. Natl. Acad. Sci. USA* 105: 3035–3040.
34. Kurz, S. K., and M. J. Reddehase. 1999. Patchwork pattern of transcriptional reactivation in the lungs indicates sequential checkpoints in the transition from murine cytomegalovirus latency to recurrence. *J. Virol.* 73: 8612–8622.
35. Munks, M. W., K. S. Cho, A. K. Pinto, S. Sierro, P. Klenerman, and A. B. Hill. 2006. Four distinct patterns of memory CD8 T cell responses to chronic murine cytomegalovirus infection. *J. Immunol.* 177: 450–458.
36. van Oosterwijk, M. F., H. Juwana, R. Arens, K. Tesselaar, M. H. van Oers, E. Eldering, and R. A. van Lier. 2007. CD27-CD70 interactions sensitise naive CD4+ T cells for IL-12-induced Th1 cell development. *Int. Immunol.* 19: 713–718.
37. van Gisbergen, K. P., R. W. van Olffen, J. van Beek, K. F. van der Sluijs, R. Arens, M. A. Nolte, and R. A. van Lier. 2009. Protective CD8 T cell memory is impaired during chronic CD70-driven costimulation. *J. Immunol.* 182: 5352–5362.
38. Tesselaar, K., R. Arens, G. M. van Schijndel, P. A. Baars, M. A. van der Valk, J. Borst, M. H. van Oers, and R. A. van Lier. 2003. Lethal T cell immunodeficiency induced by chronic costimulation via CD27-CD70 interactions. *Nat. Immunol.* 4: 49–54.
39. Pipkin, M. E., J. A. Sacks, F. Cruz-Guilloty, M. G. Lichtenheld, M. J. Bevan, and A. Rao. 2010. Interleukin-2 and inflammation induce distinct transcriptional programs that promote the differentiation of effector cytolytic T cells. *Immunity* 32: 79–90.
40. Kalia, V., S. Sarkar, S. Subramaniam, W. N. Haining, K. A. Smith, and R. Ahmed. 2010. Prolonged interleukin-2Ralpha expression on virus-specific CD8+ T cells favors terminal-effector differentiation in vivo. *Immunity* 32: 91–103.
41. Berard, M., K. Brandt, S. Bulfone-Paus, and D. F. Tough. 2003. IL-15 promotes the survival of naive and memory phenotype CD8+ T cells. *J. Immunol.* 170: 5018–5026.
42. Huntington, N. D., H. Puthalakath, P. Gunn, E. Naik, E. M. Michalak, M. J. Smyth, H. Tabarias, M. A. Degli-Esposti, G. Dewson, S. N. Willis, et al. 2007. Interleukin 15-mediated survival of natural killer cells is determined by interactions among Bim, Noxa and Mcl-1. *Nat. Immunol.* 8: 856–863.
43. Pellegrini, M., G. Belz, P. Bouillet, and A. Strasser. 2003. Shutdown of an acute T cell immune response to viral infection is mediated by the proapoptotic Bcl-2 homology 3-only protein Bim. *Proc. Natl. Acad. Sci. USA* 100: 14175–14180.
44. Sallusto, F., A. Lanzavecchia, K. Araki, and R. Ahmed. 2010. From vaccines to memory and back. *Immunity* 33: 451–463.
45. Wensveen, F. M., K. P. van Gisbergen, and E. Eldering. 2012. The fourth dimension in immunological space: how the struggle for nutrients selects high-affinity lymphocytes. *Immunol. Rev.* 249: 84–103.
46. Weant, A. E., R. D. Michalek, I. U. Khan, B. C. Holbrook, M. C. Willingham, and J. M. Grayson. 2008. Apoptosis regulators Bim and Fas function concurrently to control autoimmunity and CD8+ T cell contraction. *Immunity* 28: 218–230.
47. Hutcheson, J., J. C. Scatizzi, A. M. Siddiqui, G. K. Haines, III, T. Wu, Q. Z. Li, L. S. Davis, C. Mohan, and H. Perlman. 2008. Combined deficiency of proapoptotic regulators Bim and Fas results in the early onset of systemic autoimmunity. *Immunity* 28: 206–217.
48. Hughes, P. D., G. T. Belz, K. A. Fortner, R. C. Budd, A. Strasser, and P. Bouillet. 2008. Apoptosis regulators Fas and Bim cooperate in shutdown of chronic immune responses and prevention of autoimmunity. *Immunity* 28: 197–205.
49. Nolte, M. A., R. W. van Olffen, K. P. van Gisbergen, and R. A. van Lier. 2009. Timing and tuning of CD27-CD70 interactions: the impact of signal strength in setting the balance between adaptive responses and immunopathology. *Immunol. Rev.* 229: 216–231.